

# Electrostatic Contribution to Twist Rigidity of DNA

Farshid Mohammad-Rafiee and Ramin Golestanian

*Institute for Advanced Studies in Basic Sciences, Zanjan 45195-159, Iran*

(November 4, 2018)

The electrostatic contribution to twist rigidity of DNA is studied, and it is shown that the Coulomb self-energy of the double-helical sugar-phosphate backbone contributes considerably to twist rigidity of DNA—the electrostatic twist rigidity of DNA is found as  $C_{\text{elec}} \approx 5$  nm, which makes up about 7% of its total twist rigidity ( $C_{\text{DNA}} \approx 75$  nm). The electrostatic twist rigidity is found, however, to only weakly depend on the salt concentration, because of a competition between two different screening mechanisms: (1) Debye screening by the salt ions in the bulk, and (2) structural screening by the periodic charge distribution along the backbone of the helical polyelectrolyte. It is found that depending on the parameters, the electrostatic contribution could stabilize or destabilize the structure of a helical polyelectrolyte.

Pacs numbers: 87.15.-v, 36.20.-r, 61.41.+e

## I. INTRODUCTION

Genetic information in living cells is carried in the double-helical linear sequence of nucleotides in DNA. The DNA double-helix can be found in several forms that differ from each other in the geometrical characteristics such as diameter and handedness. Under normal physiological conditions, DNA adopts the B-form, in which it consists of two helically twisted sugar-phosphate backbones with a diameter 2.4 nm, which are stuffed with base pairs and are located asymmetrically with respect to each other as characterized by the presence of major and minor grooves. The helix is right-handed with 10 base pairs per turn, and the pitch of the helix is 3.4 nm [1].

It is well known that above pH 1 each phosphate group in DNA has a negative charge [2], which renders the polymer stiff due to the electrostatic repulsion between these groups. The presence of neutralizing counterions and salt in the solvent screens the electrostatic repulsion, thereby leading to an effective way of controlling the stiffness of polyelectrolytes via the ionic strength of the solution. To account for the electrostatic stiffening, Odijk [3], and Skolnick and Fixman [4] have adopted an effective wormlike chain description for the bending elasticity of stiff polyelectrolytes, and have calculated the correction to the persistence length due to the electrostatic interactions. The so-called electrostatic persistence length is found to be proportional to the square of the Debye screening length, implying that the stiffness of polyelectrolytes such as DNA should be very sensitive to salt concentration [5]. While there are experiments that measure the electrostatic contribution to the bending rigidity of DNA in various salt concentrations [6,7], it is generally believed that changing the ionic strength has no significant effect on the rigidity of DNA under most physiologically relevant conditions [8]. Hence, in this so-called salt saturation limit, the bending rigidity of DNA is en-

tirely due to the mechanical stiffness of the double-helical backbone.

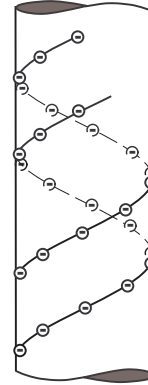


FIG. 1. The schematic picture of double-helical B-DNA with the negative charges lying on the sugar-phosphate backbone in a periodic manner.

Similar studies have shown that the twist rigidity of DNA is also relatively insensitive to the ionic strength of the solution [9]. This experimental finding is usually explained by saying that (unlike bending) twisting a polyelectrolyte does not change the distance between the different charges on its backbone appreciably, and thus it is not affected by electrostatic interactions [10]. Here, we set out to revisit this line of argument and attempt to account for the above experimental observation from a different point of view. We consider the electrostatic self-interaction of the double-helical sugar-phosphate backbone (see Fig. 1) and show that the periodic arrangement of the charge distribution effectively screens the electrostatic interaction with the screening length given by the pitch of the DNA. In other words, corresponding to such a periodic charge distribution, there are two competing screening lengths: (1) the Debye screening length of the

bulk solution  $\kappa^{-1}$  that is controlled by the ionic strength, and (2) the period of the charge distribution  $P$ , and it is the smaller of these two lengths that controls the range of Coulomb interaction. We find that electrostatic interactions make an appreciable contribution to the twist rigidity of DNA, although it depends only weakly on the Debye screening length as long as this length is larger than the DNA pitch. We study the effect of various geometrical parameters such as the diameter of the double-helix, the distance between the two helices, and the pitch, as well as the Debye screening length, on the electrostatic contribution to twist rigidity and show that it can be both positive and negative depending on the values of these parameters. The results are summarized in Fig. 2, where a diagram is sketched in the parameter space delineating all the different regimes.

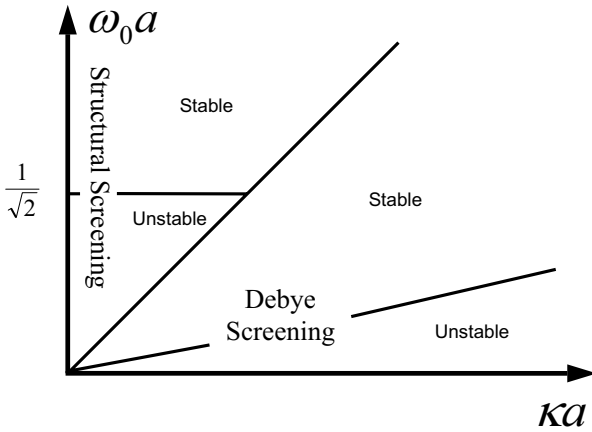


FIG. 2. The diagram delineating the different regimes in the parameter space of a helical polyelectrolyte, where  $\omega_0 = 2\pi/P$ , and  $a$  is the radius of the helix. The line separating the two screening regimes has slope one, whereas the slope of the boundary denoting the onset of instability in the Debye screening regime is set by the inverse of a cutoff number  $n_c$  (see below).

The rest of paper is organized as follows: Section II describes the model that is used to study the electrostatic contribution to twist rigidity of DNA, followed by the presentation of the results in Sec. III. Finally, Sec. IV concludes the paper, while some details of the calculations appear in three Appendices.

## II. THE MODEL

To study the effect of electrostatic interactions on the twist rigidity of DNA, we consider a simple model in

which the sugar-phosphate charged backbone of each DNA strand is assumed to wrap around a cylinder of radius  $a$  in a helical manner, as shown in Fig. 1. The double-helix can then be viewed as a cylinder with a surface charge density  $\sigma(z, \theta)$  corresponding to the negative charges, whose electrostatic self-energy can be calculated as

$$E_{\text{elec}} = \frac{a^2}{2} \int dz dz' \int_0^{2\pi} d\theta d\theta' \sigma(z, \theta) \sigma(z', \theta') \times V_{\text{DH}}(|\vec{r}(z, \theta) - \vec{r}(z', \theta')|), \quad (1)$$

where  $\vec{r}(z, \theta)$  parameterizes the position on the surface of the cylinder with  $z$  being the coordinate along the axis and  $\theta$  being the polar angle. The effective pair potential between two charges in the solution is given by the Debye-Hückel interaction [11]

$$V_{\text{DH}}(r) = k_{\text{B}} T \frac{\ell_{\text{B}}}{r} e^{-\kappa r}, \quad (2)$$

where  $\ell_{\text{B}} = e^2/(\epsilon k_{\text{B}} T)$  is the Bjerrum length, and  $\kappa^{-1}$  is the Debye screening length, defined via [5]

$$\kappa^2 = 4\pi\ell_{\text{B}} \sum_i Z_i^2 c_i, \quad (3)$$

where  $Z_i$  and  $c_i$  are the valence and the concentration of the salt species  $i$ , respectively, and summation holds over the ionic species in the solution.

Due to the helical structure of DNA,  $\sigma(z, \theta)$  is a doubly periodic function, namely,  $\sigma(z, \theta) = \sigma(z + P, \theta) = \sigma(z, \theta + 2\pi)$ , where  $P$  is the helix pitch. Therefore, it is convenient to write  $\sigma(z, \theta)$  in the Fourier space as

$$\sigma(z, \theta) = \sum_{m,n} \sigma_{mn} e^{i \frac{2\pi m}{P} z + in\theta} \quad (4)$$

where,  $m$  and  $n$  are integer numbers.

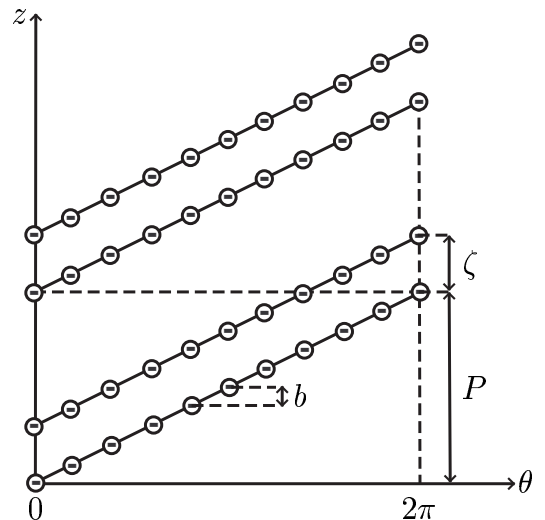


FIG. 3. The schematic picture of the surface charge distribution of B-DNA. The geometrical parameters of DNA have been shown in the picture:  $b$  is the vertical distance between two successive charges on each strand,  $\zeta$  is the distance between the two strands along the  $z$ -axis (given by the width of the minor groove in B-DNA), and  $P$  is the pitch of the helix.

Making use of the periodicity of the charge distribution, one can simplify the form of the electrostatic self-energy of Eq. (1) using the Fourier representation of the screened Coulomb interaction. After some manipulation, whose details can be found in Appendix A, one finds

$$\beta E_{\text{elec}} = 4\pi^2 \ell_B L a^2 \sum_{m,n} |\sigma_{m,n}|^2 I_n \left( \sqrt{(\kappa a)^2 + (na\omega_0)^2} \right) \times K_n \left( \sqrt{(\kappa a)^2 + (na\omega_0)^2} \right), \quad (5)$$

where  $\beta = 1/(k_B T)$ ,  $\omega_0 = 2\pi/P$  is the spontaneous twist of the helix, and  $L$  is the overall length of the macromolecule.

We now focus on the specific case of DNA, whose charge density  $\sigma(z, \theta)$  can be written as (see Fig. 3)

$$\sigma(z, \theta) = -\frac{P}{2\pi ab} \left[ \delta\left(z - \frac{P\theta}{2\pi}\right) + \delta\left(z - \zeta - \frac{P\theta}{2\pi}\right) \right], \quad (6)$$

where  $b$  is the vertical distance between two charges in a strand, and  $\zeta$  is the distance between the two strands along the  $z$  direction, as shown in Fig. 3. Note that

$$\int_0^P dz \int_0^{2\pi} ad\theta \sigma(z, \theta) = -\frac{2P}{b}, \quad (7)$$

yields the number of charges in each repeat unit of DNA. The Fourier transform of the charge density  $\sigma_{m,n}$  can now be calculated from Eqs. (4) and (6) as

$$\sigma_{m,n} = -\frac{1}{2\pi ab} \delta_{m,-n} [1 + e^{in\omega_0\zeta}], \quad (8)$$

using which the electrostatic self-energy of the double-helical DNA can be calculated (from Eq. (5)) as

$$\beta E_{\text{elec}} = \frac{4\ell_B L}{b^2} \sum_{n=0}^{\infty'} (1 + \cos n\omega_0\zeta) I_n \left( \sqrt{(\kappa a)^2 + (na\omega_0)^2} \right) \times K_n \left( \sqrt{(\kappa a)^2 + (na\omega_0)^2} \right), \quad (9)$$

where the prime indicates that the  $n = 0$  term should be counted with a prefactor of  $1/2$ .

To calculate the contribution to twist rigidity from the above Coulomb interaction, we impose an additional uniform twist of  $\Omega$  in the double-helix and calculate the change in the self-energy, i.e.  $\beta E_{\text{elec}}(\omega_0 + \Omega) - \beta E_{\text{elec}}(\omega_0)$ . Expanding the energy change in powers of  $\Omega$ , we can then read off the electrostatic twist rigidity as

$$C_{\text{elec}} = \frac{1}{L} \frac{\partial^2 \beta E_{\text{elec}}}{\partial \Omega^2}, \quad (10)$$

subject to the constraint that the relative positioning of the two helical strands should not alter upon deformation, and thus we should assume that the parameter  $\zeta$  changes accordingly to  $\zeta'$  such that  $(\omega_0 + \Omega)\zeta' = \omega_0\zeta$ .

### III. THE RESULTS

Under normal physiological conditions,  $\kappa \approx 1 \text{ nm}^{-1}$  and the spontaneous twist of B-DNA is  $\omega_0 = 1.85 \text{ nm}^{-1}$ . Since the closed form calculation of  $C_{\text{elec}}$  from Eqs. (9) and (10) is cumbersome, we choose to expand the modified Bessel functions  $I_n$  and  $K_n$  to fourth order in  $(\kappa a)/(na\omega_0)$ . This approximation appears to yield sufficient accuracy for the experimentally relevant range of parameters.

It is convenient to use the asymptotic forms of  $I_n(nx)$  and  $K_n(nx)$  for sufficiently large  $n$ . We find that  $I_n(nx)K_n(nx) = \frac{1}{2n} \frac{1}{\sqrt{1+x^2}} + O(\frac{1}{n^{2+\delta}})$  with  $\delta \geq 0$ , and observe that to a good approximation one can just use the relevant asymptotic forms of  $I_n$  and  $K_n$  for  $n \geq 2$ , in calculating the electrostatic twist rigidity (see Appendix B for details). We find

$$C_{\text{elec}} = \frac{2\ell_B a^2}{b^2} (1 + \cos \omega_0 \zeta) \times [f_0(a\omega_0) - f_2(a\omega_0)(\kappa a)^2 + f_4(a\omega_0)(\kappa a)^4] + \frac{2\ell_B a^2}{b^2} \frac{(2a^2\omega_0^2 - 1)}{(a^2\omega_0^2 + 1)^{5/2}} \sum_{n=2}^{\infty} \frac{1}{n} (1 + \cos n\omega_0\zeta), \quad (11)$$

where  $f_0(x)$ ,  $f_2(x)$ , and  $f_4(x)$  are functions defined in Appendix C. In the summation term in Eq. (11) above, where we have used the asymptotic forms of the Bessel functions, no dependence on  $\kappa$  remains and only the structural parameters of DNA such as  $a$  and  $\omega_0$  enter. The summation diverges as  $1/n$ , and needs to be regularized with a cutoff for  $n$ , which can be estimated as  $n_c = 2\pi a/t$ , where  $t$  is set by the thickness of each strand. Then, Eq. (11) can be written as

$$C_{\text{elec}} = \frac{2\ell_B a^2}{b^2} (1 + \cos \omega_0 \zeta) \times [f_0(a\omega_0) - f_2(a\omega_0)(\kappa a)^2 + f_4(a\omega_0)(\kappa a)^4] + \frac{2\ell_B a^2}{b^2} \frac{(2a^2\omega_0^2 - 1)}{(a^2\omega_0^2 + 1)^{5/2}} \times \left[ \gamma + \ln \frac{n_c}{2 \sin(\omega_0\zeta/2)} - (1 + \cos \omega_0\zeta) \right], \quad (12)$$

where  $\gamma = 0.577216$  is the Euler's constant. Note that the above result, as we have already mentioned, is only valid for  $\kappa < \omega_0$ .

Let us first evaluate the overall magnitude of the electrostatic twist rigidity, as given by Eq. (12). For B-DNA, we have  $a = 1.2 \text{ nm}$ ,  $\omega_0 = 1.85 \text{ nm}^{-1}$ ,  $b = 3.4 \text{ \AA}$

and  $\zeta = 1.13$  nm [2], and the Bjerrum length is given as  $\ell_B = 7.1$  Å. Using these parameters, we find  $C_0 = 174$  Å, which is relatively large. To estimate  $n_c$  for B-DNA, we use  $t \approx 5$  Å, which gives  $n_c \approx 15$ . Using these estimates and  $\kappa \approx 1$  nm<sup>-1</sup>, Eq. (12) yields  $C_{\text{elec}} = 46$  Å at physiological salt concentration.

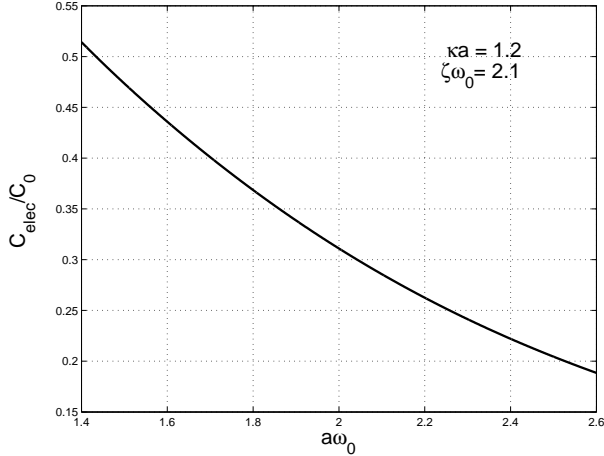


FIG. 4.  $C_{\text{elec}}/C_0$  as a function of  $a\omega_0$ . This plot corresponds to  $\kappa a = 1.2$  and  $\zeta\omega_0 = 2.1$ .

To study the effect of various parameters, namely, the spontaneous twist, the diameter, and the asymmetry of the double-helix, as well as the salt concentration, we choose to work with three dimensionless parameters of  $a\omega_0$ ,  $\kappa a$ , and  $\zeta\omega_0$ . In Fig. 4, the behaviour of  $C_{\text{elec}}$  is shown as a function of  $a\omega_0$  for  $\kappa a = 1.2$  and  $\zeta\omega_0 = 2.1$ . The domain for  $a\omega_0$  is chosen such that the condition  $\kappa < \omega_0$  is satisfied and Eq. (12) is valid. The plot shows that for sufficiently high salt concentration, the electrostatic torsional stiffness decreases as the spontaneous twist of the double-helix increases.

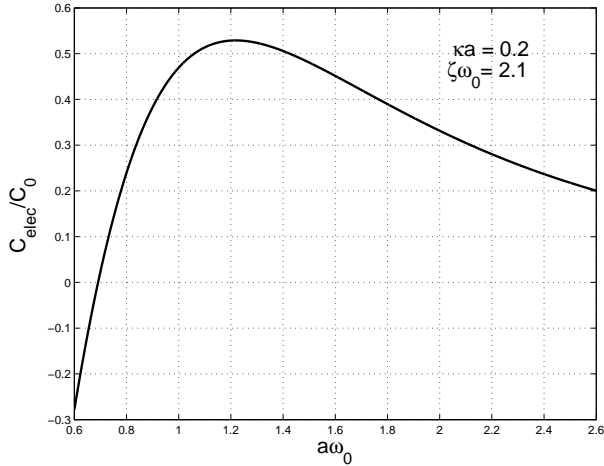


FIG. 5.  $C_{\text{elec}}/C_0$  as a function of  $a\omega_0$ . This plot corresponds to  $\kappa a = 0.2$  and  $\zeta\omega_0 = 2.1$ .

For sufficiently low salt concentration, however, it appears that the behavior is not always monotonic as shown in Fig. 5, where  $C_{\text{elec}}$  is plotted as a function of  $a\omega_0$  for  $\kappa a = 0.2$  and  $\zeta\omega_0 = 2.1$ . Interestingly, one can see that  $C_{\text{elec}}$  can even become negative, due to the fact in Eq. (12) the first term becomes relatively weak for low salt concentrations and the second term that is dominant changes sign for  $a\omega_0 < 1/\sqrt{2}$ .

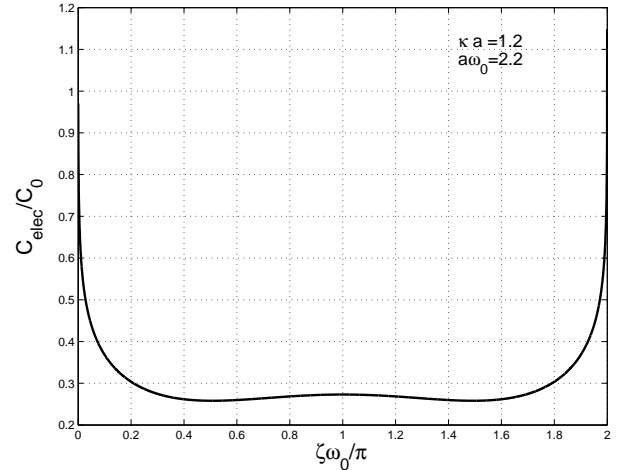


FIG. 6.  $C_{\text{elec}}/C_0$  as a function of  $\zeta\omega_0/\pi$ . This plot corresponds to  $\kappa a = 1.2$  and  $a\omega_0 = 2.2$ .

In Fig. 6, the dependence of  $C_{\text{elec}}$  is shown on the asymmetry parameter  $\zeta\omega_0$  for  $\kappa a = 1.2$  and  $a\omega_0 = 2.2$ . One observes that for the relatively large window of  $0.4\pi \leq \zeta\omega_0 \leq 1.6\pi$ ,  $C_{\text{elec}}$  is almost constant, and is thus not sensitive to the relative positioning of the two strands. For  $\zeta\omega_0 = 0$  and  $2\pi$ , a divergence sets in due to the fact that the charges on the two strands develop contacts with each other.

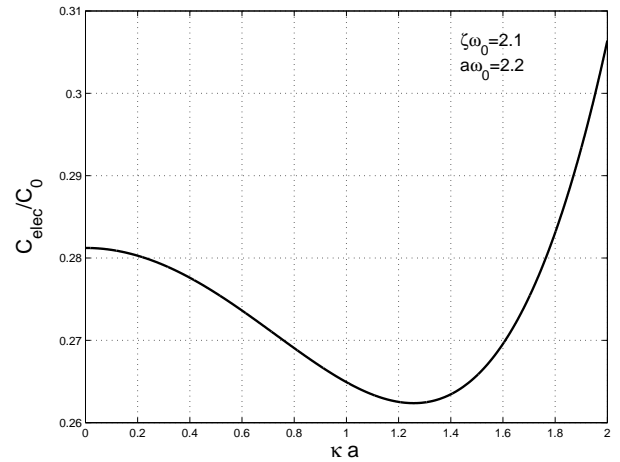


FIG. 7.  $C_{\text{elec}}/C_0$  as a function of  $\kappa a$ . This plot corresponds to  $\zeta\omega_0 = 2.1$  and  $a\omega_0 = 2.2$ .

Finally, the behavior of  $C_{\text{elec}}$  is shown in Fig. 7 as a function of  $\kappa a$  for  $\zeta\omega_0 = 2.1$  and  $a\omega_0 = 2.2$ . The dependence on the Debye screening parameter in Eq. (12) comes only from the first term, where the negative sign of the coefficient of  $(\kappa a)^2$  causes a dip in the plot for  $C_{\text{elec}}$  around  $\kappa a \approx 1.3$ , which by chance corresponds to the normal physiological salt concentration. However, as can be seen from Fig. 7, the dependence of the electrostatic twist rigidity on  $\kappa a$  is extremely weak as long as  $\kappa < \omega_0$ , which is a manifestation of the fact that screening is controlled by the periodic charge distribution and the effective screening length is set by the pitch  $P$  that is shorter than  $\kappa^{-1}$  in this regime.

It is worth saying a few words about the other limit where  $\kappa > \omega_0$ , corresponding to high salt concentration. In Eq. (9), one can manifestly see that in the  $n$ th term in the series there is a competition between  $\kappa$  and  $n\omega_0$  to control the screening. If the salt concentration is so high that we have  $\kappa > n_c\omega_0$ , the periodic structure plays no role and screening is entirely controlled by the Debye screening in the bulk. For relatively strong Debye screening when  $\kappa a > 1$ , we can use the simple asymptotic forms of the Bessel functions and find an asymptotic expression for the electrostatic twist rigidity as

$$C_{\text{elec}} = \frac{2\ell_B a^2}{b^2} \sum_{n=1}^{n_c} (1 + \cos n\omega_0\zeta) \frac{n^2[2(na\omega_0)^2 - (\kappa a)^2]}{[(\kappa a)^2 + (na\omega_0)^2]^{5/2}}. \quad (13)$$

This expression can be used for the region  $\kappa > \omega_0$ , where it predicts  $C_{\text{elec}} > 0$  for  $\kappa < s\omega_0$ , and  $C_{\text{elec}} < 0$  for  $\kappa > s\omega_0$ , for a value of  $s \approx n_c$ .

#### IV. DISCUSSION

For a polyelectrolyte with a periodic spatial charge distribution, such as the double-helical structure of DNA, there are two competing mechanisms for screening the electrostatic self-interaction and its contribution to twist rigidity, namely, the *Debye screening* due to the free ions in the solution, and the *structural screening* caused by the periodic structure of the charge distribution. While the screening length for the former case is set by the Debye length  $\kappa^{-1}$ , it is set by the period  $P$  of the charge distribution in the latter, and the dominant mechanism corresponds to the one with the shorter screening length.

It appears that the contribution of electrostatic interactions to twist rigidity can be both negative and positive, depending on the parameters. The negative values for the electrostatic torsional stiffness could lead to instability in the structure of the helical polyelectrolyte, depending on whether the mechanical structure of the macromolecule can counter-balance the effect of the electrostatic instability. We have used this criterion in Fig. 2 to summarize these different regimes in the parameter space. Considering that a helical polyelectrolyte seems to

be the general structure of many stiff biopolymers (such as DNA and actin) it will be interesting to know which helical configurations can in principle lead to stable structures, and which ones cannot. This could especially be important in the case of biopolymers that self-assemble through polymerization processes, such as actin, where such energetic considerations could hamper or favor the polymerization process.

The twist rigidity of B-DNA is believed to be roughly 75 nm [13], which should be thought of as the sum of the mechanical and the electrostatic contributions:  $C = C_{\text{mech}} + C_{\text{elec}}$ . Our estimate of  $C_{\text{elec}} \approx 5$  nm reveals that about 7% of the twist rigidity of DNA is due to electrostatic interactions. This result is more or less independent of the salt concentration, as the dependence of  $C_{\text{elec}}$  to salt concentration is very weak. For example, the difference between  $C_{\text{elec}}$  at zero and very high salt concentration is about 3.5 Å. Therefore  $\Delta C_{\text{elec}}/C = 0.5\%$ , which is very small. While this naturally explains why in the experiments no sensitivity on the salt concentration has been observed, it certainly does not mean that the electrostatic contribution to  $C$  is negligible.

In the above analysis we have assumed that imposing a finite angle of twist between the two ends of a helical polyelectrolyte leads to a uniform twist. This is analogous to the assumption of a uniform bending made by Odijk when calculating the electrostatic bending rigidity, and presumably holds true when the effective elasticity due to electrostatics is local. In Ref. [14], this assumption has been scrutinized and it has been shown that this assumption is valid provided one of these conditions hold: (1) the polyelectrolyte segment is long, (2) the Debye screening is strong, (3) the charging is weak, or (4) the mechanical stiffness of the polyelectrolyte is larger than the electrostatic contribution. We expect the same argument to hold true for the twist rigidity as well. Since for the case of DNA we have shown that the mechanical twist rigidity is much larger than the electrostatic contribution, we can safely assume that the twist is uniform.

In conclusion, we have studied the electrostatic contribution to twist rigidity of DNA, taking into account its dependence on salt concentration in the solvent. We have shown that there is a non-negligible electrostatic contribution to twist rigidity, which varies very slowly by changing the salt concentration in the solution. By changing the geometrical parameters of the helix and the Debye screening length, the electrostatic twist rigidity can change sign and become negative, implying that a helical structure could be both stable as well as unstable configuration for a helical polyelectrolyte. We finally note that the present analysis can be also applied to other biopolymers such as F-actin.

## ACKNOWLEDGMENTS

We are grateful to T.B. Liverpool for interesting discussions and comments.

## APPENDIX A: COULOMB ENERGY IN FOURIER SPACE

Due to the periodicity of the charge distribution, it is convenient to calculate the electrostatic self energy in Eq. (1) in Fourier space. We start from the Fourier representation of the screened Debye-Hückel interaction in Eq. (2):

$$\beta E_{\text{elec}} = \frac{a^2}{2} \int \frac{d^3 k}{(2\pi)^3} \int dz dz' \int_0^{2\pi} d\theta d\theta' \sigma(z, \theta) \sigma(z', \theta') \times \frac{4\pi \ell_B}{k^2 + \kappa^2} e^{i\vec{k} \cdot [\vec{r}(z, \theta) - \vec{r}(z', \theta')]} \quad (\text{A1})$$

Using the cylindrical coordinates, we can write  $\vec{r}(z, \theta) = z\hat{z} + a(\cos\theta \hat{x} + \sin\theta \hat{y})$ , which in conjunction with  $\vec{k} = k_z \hat{z} + k_\perp (\cos\phi \hat{x} + \sin\phi \hat{y})$ , yields

$$\beta E_{\text{elec}} = \frac{\ell_B a^2}{2} \int dz dz' \int_0^{2\pi} d\theta d\theta' \times \int_{-\infty}^{+\infty} \frac{dk_z}{2\pi} \int_0^\infty \frac{k_\perp dk_\perp}{(2\pi)^2} \int_0^{2\pi} d\phi \times \sum_{m, n} \sum_{m', n'} \sigma_{m, n} \sigma_{m', n'} \frac{4\pi}{k_z^2 + k_\perp^2 + \kappa^2} \times e^{i(\frac{2\pi}{P}m + k_z)z + in\theta + ik_\perp a \cos(\phi - \theta)} \times e^{i(\frac{2\pi}{P}m' - k_z)z' + in'\theta' - ik_\perp a \cos(\phi - \theta')}. \quad (\text{A2})$$

After integration over  $z$ ,  $z'$ , and  $k_z$ , we find

$$\beta E_{\text{elec}} = \frac{\ell_B a^2}{2} \int_0^{2\pi} d\theta d\theta' d\phi \int_0^\infty \frac{k_\perp dk_\perp}{(2\pi)^2} \times \sum_{m, n} \sum_{m', n'} \sigma_{m, n} \sigma_{m', n'} \frac{4\pi L \delta_{m, -m'}}{(\frac{2\pi}{P}m)^2 + k_\perp^2 + \kappa^2} \times e^{i(n\theta + n'\theta') + ia k_\perp [\cos(\phi - \theta) - \cos(\phi - \theta')]} \quad (\text{A3})$$

By defining  $\theta = \theta_1 + \phi$  and  $\theta' = \theta_2 + \phi$ , the integration over the three angles in Eq. (A3) can be performed as

$$\int d\theta d\theta' d\phi e^{i(n\theta + n'\theta') + ia k_\perp [\cos(\phi - \theta) - \cos(\phi - \theta')]} = (2\pi)^3 \delta_{n, -n'} [J_n(k_\perp a)]^2, \quad (\text{A4})$$

to yield

$$\beta E_{\text{elec}} = 4\pi^2 \ell_B L a^2 \sum_{m, n} |\sigma_{m, n}|^2 \times \int_0^\infty dk_\perp k_\perp \frac{J_n^2(k_\perp a)}{(\frac{2\pi}{P}m)^2 + k_\perp^2 + \kappa^2}. \quad (\text{A5})$$

Performing the final integration over  $k_\perp$  using [12]

$$\int_0^\infty \frac{x}{x^2 + h^2} [J_\nu(x)]^2 dx = I_\nu(h) K_\nu(h), \quad (\text{A6})$$

we obtain the result quoted in Eq. (5).

## APPENDIX B: ASYMPTOTIC FORMS OF THE BESSEL FUNCTIONS

In this Appendix, the asymptotic forms of  $I_n(nx)$  and  $K_n(nx)$ , for large  $n$  are derived. We use the integral representation of these functions:

$$I_n(nx) = \frac{1}{\pi^{\frac{1}{2}}(n - \frac{1}{2})!} \left(\frac{nx}{2}\right)^n \int_{-1}^{+1} dp e^{nxp} (1 - p^2)^{n - \frac{1}{2}} \\ K_n(nx) = \frac{\pi^{\frac{1}{2}}}{(n - \frac{1}{2})!} \left(\frac{nx}{2}\right)^n \int_1^\infty dp e^{-nxp} (p^2 - 1)^{n - \frac{1}{2}}. \quad (\text{B1})$$

Let us first consider the case of  $I_n(nx)$ . We denote

$$Q \equiv \int_{-1}^{+1} dp e^{nxp} (1 - p^2)^{n - \frac{1}{2}} = \int_{-1}^{+1} dp e^{g(p)}, \quad (\text{B2})$$

and expand  $g(p)$  around  $p_0$ , the position of its maximum, to second order of  $(p - p_0)$ , as

$$g(p) \simeq g(p_0) + \frac{1}{2} f''(p_0) (p - p_0)^2 \\ = nx p_0 + \left(n - \frac{1}{2}\right) \ln(1 - p_0^2) \\ - \left(n - \frac{1}{2}\right) \frac{1 + p_0^2}{(1 - p_0^2)^2} (p - p_0)^2, \quad (\text{B3})$$

where

$$p_0 = \frac{-1 + \sqrt{1 + x^2}}{x} + \frac{1}{2nx} \left(1 + \frac{1}{\sqrt{1 + x^2}}\right). \quad (\text{B4})$$

Using this form for  $g(p)$ ,  $Q$  can be found as

$$Q \simeq \frac{1 - p_0^2}{\sqrt{n(1 + p_0^2)}} e^{n x p_0 + (n - \frac{1}{2}) \ln(1 - p_0^2)}. \quad (\text{B5})$$

Finally, using the Stirling's formula for  $n!$ , we find

$$I_n(nx) \simeq \frac{1}{\sqrt{2\pi}} \frac{1 - p_0^2}{\sqrt{n(1 + p_0^2)}} \\ \times e^{(n - \frac{1}{2}) \ln(1 - p_0^2) + n x p_0 + n(1 + \ln \frac{x}{2}) + \frac{1}{24n}}. \quad (\text{B6})$$

Using a similar treatment, we find the large  $n$  asymptotic behavior for  $K_n(nx)$ , as

$$K_n(nx) \simeq \frac{1}{\sqrt{2n}} \frac{p_0'^2 - 1}{\sqrt{n(1+p_0'^2)}} \times e^{(n-\frac{1}{2}) \ln(p_0'^2 - 1) - nx p_0' + n(1 + \ln \frac{x}{2}) + \frac{1}{24n}}, \quad (\text{B7})$$

where

$$p_0' = \frac{1 + \sqrt{1+x^2}}{x} - \frac{1}{2nx} \left( 1 + \frac{1}{\sqrt{1+x^2}} \right). \quad (\text{B8})$$

By using these relations for  $I_n(nx)$  and  $K_n(nx)$ , we find

$$I_n(nx)K_n(nx) = \frac{1}{2\sqrt{1+x^2}} \frac{1}{n} + O\left(\frac{1}{n^{2+\delta}}\right), \quad (\text{B9})$$

where  $\delta \geq 0$ .

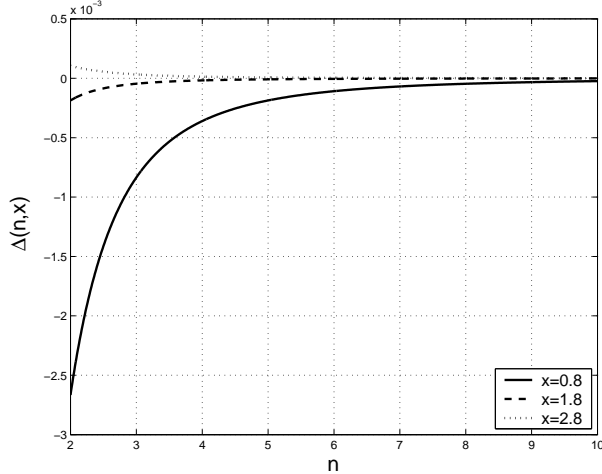


FIG. 8. Difference between the asymptotic form of  $I_n(nx)K_n(nx)$  and its exact value as a function of  $n$  for several values of  $x$ . The solid line corresponds to  $x = 0.8$ , the dashed line corresponds to  $x = 1.8$ , and the dotted line corresponds to  $x = 2.8$ . The difference is less than 0.25%.

We define  $\Delta(n, x) \equiv I_n(nx)K_n(nx) - \frac{1}{2n\sqrt{1+x^2}}$ , and in Fig. 8 show the behaviour of  $\Delta(n, x)$  as a function of  $n$  for several values of  $x$ . As can be seen, the difference is less than 0.25% in the worst case, which implies that the asymptotic form of  $I_n(nx)K_n(nx)$  for  $n \geq 2$  can be used as a good approximation for the range of  $x$  we are interested in.

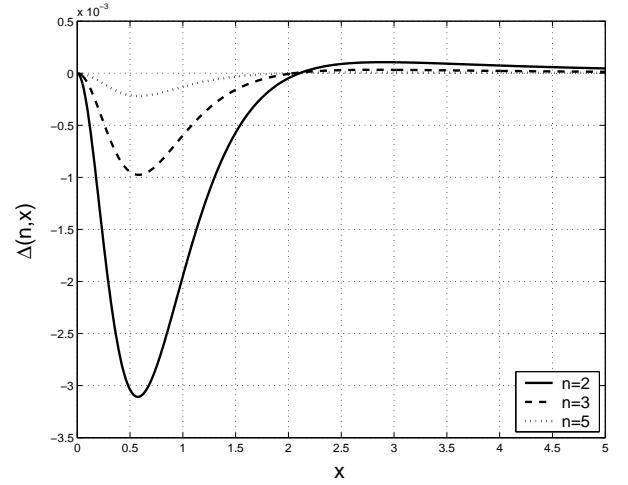


FIG. 9. Difference between the asymptotic form of  $I_n(nx)K_n(nx)$  and its exact value as a function of  $x$  for different values of  $n$ . The solid line corresponds to  $n = 2$ , the dashed line corresponds to  $n = 3$ , and the dotted line corresponds to  $n = 5$ . The difference is less than 0.3%.

In Fig. 9, we show the behaviour of  $\Delta(n, x)$  as a function of  $x$  for different values of  $n$ . This plot shows that for  $n \geq 2$ , the difference goes to zero as  $x$  increases.

### APPENDIX C: THE EXPLICIT FORMS OF THE AUXILIARY FUNCTIONS

In this Appendix, we give the explicit forms of the auxiliary functions used in Eqs. (11) and (12) above. The function  $f_0(x)$  reads

$$f_0(x) = 4 \left( 1 + \frac{1}{x^2} \right) I_1(x)K_1(x) + 4I_1'(x)K_1'(x) - \frac{2}{x} [I_1(x)K_1'(x) + I_1'(x)K_1(x)], \quad (\text{C1})$$

where the prime indicates differentiation. One can show that for  $x \ll 1$  it behaves as  $f_0(x) = \ln x + O(x^2 \ln x)$ . The second function  $f_2(x)$  is written as

$$f_2(x) = -3 \left( \frac{1}{x} + \frac{1}{x^3} \right) [I_1(x)K_1'(x) + I_1'(x)K_1(x)] + \frac{1}{x} [I_1'(x)K_2'(x) - I_2'(x)K_1'(x)] + \frac{3}{x^2} [I_1(x)K_1(x) - 2I_1'(x)K_1'(x)] + \frac{3}{2x^2} [I_2'(x)K_1(x) - I_1(x)K_2'(x)] + \frac{2}{x^3} [I_1(x)K_2(x) - I_2(x)K_1(x)], \quad (\text{C2})$$

and for  $x \ll 1$  it behaves as  $f_2(x) = 1/(2x^2) - \ln x/2 + O(x^2 \ln x)$ . Finally, for  $f_4(x)$  we have

$$f_4(x) = \frac{176 + 136x^2 + 19x^4}{16x^6} I_1(x)K_1(x)$$

$$\begin{aligned}
& - \frac{7}{8x^3} [I_3(x)K_1'(x) + I_1'(x)K_3(x)] \\
& + \frac{1}{x^4} [I_2(x)K_1'(x) - I_1'(x)K_2(x)] \\
& + \frac{11 + 2x^2}{x^4} I_1'(x)K_1'(x) + \frac{1}{16x^2} I_3(x)K_3(x) \\
& + \frac{14 + 3x^2}{8x^4} [I_2'(x)K_1(x) - I_1(x)K_2'(x)] \\
& - \frac{88 + 49x^2}{8x^5} [I_1'(x)K_1(x) + I_1(x)K_1'(x)] \\
& - \frac{1}{x^5} [I_2(x)K_1(x) - I_1(x)K_2(x)], \quad (C3)
\end{aligned}$$

which behaves as  $f_4(x) = 3/(4x^4) - 1/(8x^2) + 5/64 \ln x + O(x^2 \ln x)$ , for  $x \ll 1$ . At infinity, all of these functions go to zero faster than  $1/x^2$ , with  $f_4(x)$  vanishing faster than  $f_2(x)$ , and  $f_2(x)$  faster than  $f_0(x)$ , respectively.

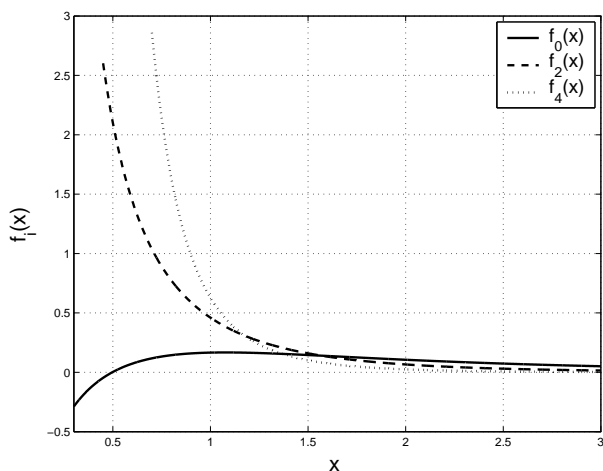


FIG. 10. The auxiliary functions  $f_0(x)$ ,  $f_2(x)$ , and  $f_4(x)$ .

- [1] B. Alberts, A. Johnson, J. Lewis, M. Raff, K. Roberts, and P. Walter, *Molecular Biology of the Cell*, (Garland, New York, 2002).
- [2] V. A. Bloomfield, D. M. Crothers, and I. Tinoco Jr., *Nucleic Acids: Structure, Properties, and Functions*, (University Science Books, Sausalito, California, 2000).
- [3] T. Odijk, *J. Polym. Sci.* **15**, 477 (1977).
- [4] J. Skolnick and M. Fixman *Macromolecules* **10**, 944 (1977).
- [5] For a review on polyelectrolyte elasticity see: J.-L. Barrat and J.-F. Joanny, *Advances in Chemical Physics: Polymeric Systems, Vol. 94* I. Prigogine and S. A. Rice. eds. (John Wiley, New York, 1996).
- [6] M. D. Wang, H. Yin, R. Landick, J. Gelles, and S. M. Block, *Biophys. J.* **72**, 1335 (1997).
- [7] C. G. Baumann, S. B. Smith, V. A. Bloomfield, and C. Bustamante, *Proc. Natl. Acad. Sci. USA* **94**, 6185 (1997).
- [8] P. J. Hagerman, *Biopolymers* **22**, 811 (1983).
- [9] W. H. Taylor and P. J. Hagerman, *J. Mol. Biol.* **212**, 363 (1990).
- [10] R. D. Kamien, T. C. Lubensky, P. Nelson, C. S. O'Hern, *Europhys. Lett.* **38**, 237 (1997).
- [11] E. J. W. Verwey and J. Th. G. Overbeek, *Theory of the Stability of Lyophobic Colloids*, (Elsevier, New York, 1948).
- [12] I. S. Gradshteyn and I. M. Ryzhik, *Table of Integrals, Series, and Products*, Six Edition (Academic Press, New York, 2000).
- [13] A. V. Vologodskii, S. D. Levene, K. V. Klenin, M. Frank-Kamenetskii, and N. R. Cozzarelli, *J. Mol. Biol.* **272**, 1224 (1992); J.F. Marko and E.D. Siggia, *Phys. Rev. E* **52**, 2912 (1995).
- [14] R. Zandi, J. Rudnick, and R. Golestanian, *Eur. Phys. J. E* **9**, 41 (2002); *Phys. Rev. E* **67**, 021803 (2003); *Phys. Rev. E*, in press (2003) (e-print cond-mat/0208178).